12th IFAC International Symposium on
Advanced Control of Chemical Processes
July 14-17, 2024. Toronto, Canada

Self-Optimizing Control for Recirculated Gas lifted Subsea Oil Well Production ⋆

Risvan Dirza * **Edmary Altamiranda** ** **Sigurd Skogestad** *

* *Department of Chemical Engineering, Norwegian University of Science and Technology, Trondheim, Norway (e-mail: risvan.dirza@ntnu.no; sigurd.skogestad@ntnu.no).*
** *Technology Department, Aker BP ASA, Norway (e-mail: edmary.altamiranda@akerbp.no)*

Abstract: Optimizing subsea oil production systems utilizing recirculated gas lift and limited produced gas treatment capacity presents challenges. Real-time optimization (RTO) is a used method for optimizing such systems, but it is restricted by the lack of reliable sensors and the high cost of developing and updating models. As a result, the RTO is typically executed infrequently, and the optimal set points are not updated in real time, leading to suboptimal plant performance over extended periods. This study implements self-optimizing control (SOC) techniques as an alternative solution that can handle frequent disturbances and drive the plant towards near-optimal performance without requiring frequent model updates or solver use. It compares different SOC structures in recirculated gas-lifted oil production optimization, their advantages, and disadvantages. The study concludes that SOC structures are an effective and suitable alternative to RTO, particularly in large and complex systems with limited measurement capabilities, given sufficient process system knowledge is considered for SOC design. This conclusion reinforces previous research, but with a more realistic case study.

Keywords: Self-optimizing control, Advanced process control, Real-time optimization, Offshore, Oil and gas,

1. INTRODUCTION

The subsea oil and gas industry has placed greater emphasis on efficient production processes while meeting safety, environmental, and cost-effectiveness requirements. This has led to the development of innovative artificial lift techniques such as gas-lifted subsea oil production optimization to increase the flow rate of oil from a reservoir. This technique involves injecting compressed gas into the wellbore to reduce the hydrostatic pressure of the fluid column, allowing the reservoir to flow more easily. The compressed gas is typically produced gas or gas injected from a separate source. Taking gas from a separate source may be *less commercially attractive* for *offshore* facilities.

Overall, a gas lift system is a forgiving method of enhanced production, in other words, even a poor gas lift design may increase production (Elldakli, 2017). However, many optimization studies have been limited by less realistic assumptions, such as a fixed separator pressure and gas lift supply from an separate source (Aamo et al., 2005; Krishnamoorthy et al., 2016), which is less likely designed for offshore facilities. Here, we consider a case of *recirculated gas lift oil production system*, which utilizes produced gas as its total gas lift supply and injects it into wells using a gas lift compressor train. This is the most practically common structure of gas lift oil production system. To improve accuracy, a dynamic separator model that considers varying pressure conditions has also been developed.

When it comes to optimizing a recirculated gas lift subsea oil production system with limited produced gas treatment capacity, one might think that numerical-based real-time optimization (RTO) completed with a dynamic estimator is the obvious solution. This method involves optimizing the process economics using rigorous steady-state models, while disturbances are estimated by the dynamic estimator (Krishnamoorthy et al., 2018; Matias and Le Roux, 2018). However, there are several challenges that this method may not be able to overcome. The challenges are as follows:

(1) Costly suitable model development for numerical solver leading to infrequent optimal set point updates: Experienced process engineers may create suitable models, but it can be time-consuming due to numerous parameter updates. Frequent optimization may not be easily performed, and regular set point updates may only occur weekly or even monthly. However, disturbances can occur more frequently, requiring fast time scale self-optimizing control (SOC) structures.
(2) Limited available measurement to estimate essential parameters such as disturbances and gradients: Accurate estimations of essential parameters such as disturbance and gradient are necessary for optimization purposes, but they may be hindered by the lack of sufficient or reliable sensors in the measurement. Thus, gradient-based SOC techniques or the use of

⋆ The authors gratefully acknowledge the financial support from SUBPRO, which is financed by the Research Council of Norway, major industry partners and NTNU.

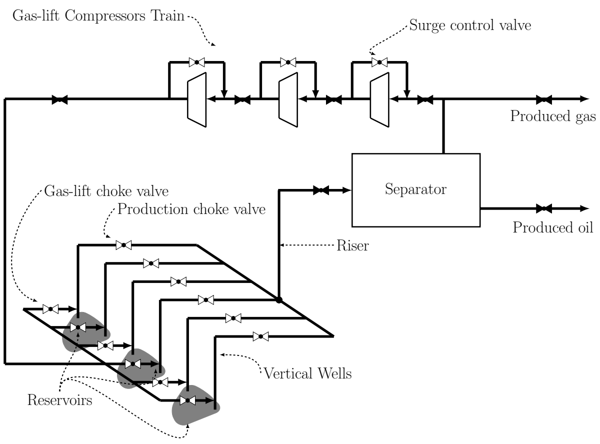

Fig. 1. The recirculated gas lift oil production system. Black valves represent pressure drop. The opening of the white valves can be manipulated in practice.

dynamic estimator may not be preferable, or their application may be limited.

(3) Numerical solvers may have issues with numerical robustness: This kind of issue may occur due to several reasons, including not having a solver-friendly model (even though it is a good model for simulation). Furthermore, some solvers may fail to find the solution due to this issue.
(4) Costly dynamic model development for dynamic estimator in large and complex systems with multiple units and different timescales can be challenging and time-consuming: This dynamic model is required for dynamic estimator, and without a good dynamic model, parameter estimation may not be accurate or may provide non-sense estimation.

Hence, alternative solutions, such as SOC, are considered to address these challenges. This work explores several potential self-optimizing control structures for recirculated gas-lifted subsea oil production systems.

2. PROBLEM DESCRIPTION

This section describes a case study designed to explore the possibility of identifying the most effective and suitable self-optimizing control structure that can maximize profits, even under conditions of reservoir uncertainty and limited produced gas treatment capacity.

2.1 Recirculated Gas Lifted Subsea Oil Production System

The recirculated gas lift oil production system is depicted in Fig. 1. The system consists of six (6) gas lifted-oil producing wells, riser, separator, gas lift compressor train (series of three centrifugal compressor), and gas lift supply line. The model is based on extensive research, modification and integration from various sources, including Gravdahl and Egeland O. (1998); Aamo et al. (2005); Cortinovis et al. (2015); Backi et al. (2018); Milosavljevic et al. (2020), to name a few. However, to maintain the focus of this work, the description of the complete model is not included in this paper. By incorporating more realistic assumptions, we aim to provide a more realistic representation of the gas lift oil production process, which has not been previously discussed to the best of the author's knowledge.

2.2 Steady-state Optimization Problem Formulation

The problem at hand involves determining the optimal gas lift valve (GLV) positions and surge control valve (SCV) positions for each gas lift compressor to maximize revenue from produced oil, minimize energy consumption of the compressor train, and satisfy operational constraints. The production choke valves (PCV) are assumed to be fixed and fully open (to hold convex problem assumption), regardless of the disturbance being considered. Additionally, fixed angular velocity is assumed for each gas lift compressor for practical reasons. The steady-state optimization problem formulation can be expressed as follows:

$$
\begin{aligned}
\min_{\mathbf{u}} \quad & J(\mathbf{u}, d) = -p_{oil} w_{os} + p_{en} \Phi_{gl} && \text{(1a)} \\
\text{s.t.} \quad & g_{z_{gl,i}}(\mathbf{u}, d) : z_{gl,i} - 1 \leq 0 \quad i = 1, \ldots, 6, && \text{(1b)} \\
& g_{z_{s,i}}(\mathbf{u}, d) : -z_{s,i} + 0 \leq 0 \quad i = 1, \ldots, 3, && \text{(1c)} \\
& g_{s_i}(\mathbf{u}, d) : s_i - \bar{s}_i \leq 0 \quad i = 1, \ldots, 3, && \text{(1d)} \\
& g(\mathbf{u}, d) : w_{gs} - \bar{w}_{gs} \leq 0 && \text{(1e)}
\end{aligned}
$$

Here, the manipulated variables (MVs) are as follows:

$$\mathbf{u} = [z_1 \ \ldots \ z_{n_\mathbf{u}}]^\top = [z_{gl,1} \ \ldots \ z_{gl,6} \ z_{s,1} \ \ldots \ z_{s,3}]^\top$$

where $z_{gl,i}$ is the position of GLV of well i, $z_{s,i}$ is the position of SCV of gas lift compressor i, and $n_\mathbf{u} = 9$ is the number of MVs. The disturbance d comes from reservoir uncertainty. The produced oil rate, produced gas rate, and maximum produced gas treatment capacity are represented by w_{os}, w_{gs}, and $\bar{w}_{gs}$, respectively. The price of oil and energy are represented by p_{oil} and p_{en}, respectively.The energy consumed by the gas lift compressor train is represented by, $\Phi_{gl} = \sum_{i=1}^{3} \Phi_{gl,i}$. The surge of gas lift compressor i is represented as s_i, and the associated limit is represented as $\bar{s}_i$. The input constraints for the GLV and SCV are shown in constraints (1b) and (1c), respectively. The surge constraint of gas lift compressor i is shown in constraint (1d), and the produced gas constraint is shown in constraint (1e).

In addition to constrained variables, we assume that the available measurements are:

$$\mathbf{y} = [p_{bh,2} \ p_{wh,2} \ p_{d,3} \ p_s]^\top$$

Here, $p_{d,3}$ represents the discharge pressure of the gas lift compressor train, and p_s represents the separator pressure. Both of them are the *artificial boundaries* in the previous studies. Meanwhile $p_{bh,2}$ and $p_{wh,2}$ are bottom hole and wellhead pressure of well 2, respectively.

2.3 The Nominal Optimal Operating Point

When the numerical solver finds the optimal solution by solving problem (1), a nominal optimal steady-state operating point can be obtained. This process most likely occur at a slow and infrequent time scale. The obtained decision/MVs associated with this nominal optimal operating point are as follows.

$$\mathbf{u}^\star = [0.88 \ 0.49 \ 1.00 \ 0.64 \ 0.60 \ 0.81 \ 0.00 \ 0.00 \ 0.00]^\top \quad (2)$$

Further, the active constraints associated with this nominal optimal operating point are $g^\star_{z_{gl,3}}$, $g^\star_{z_{s,1}}$, $g^\star_{z_{s,2}}$, $g^\star_{z_{s,3}}$, $g^\star_{s,1}$, $g^\star_{s,2}$, $g^\star_{s,3}$, and $g^\star$. It means that with a given disturbance d, optimal operation happen if constraints (1c)-(1e) are active, and the position of GLV 3 is fully open. A GLV may have a gain inversion. However, we assume that the chosen operation point is far from this occurrence.

2.4 Reservoir Uncertainty (Disturbances)

The uncertainty in the reservoir, denoted by d, is related to the gas-oil-ratio of a particular well that exhibits unstable conditions. To be specific, we assume that the disturbance is originating from well 2, and is represented by $d = GOR_2$.

Multiphase flow meter (MPFM) has recently been recommended for frequent estimation of the GOR or other parameters of a well, replacing the use of test separator. Despite its promising performance, only 3% of the 70,000 active oil producing wells worldwide have utilized MPFM (Mehdizadeh, 2007). To address the majority of the case, we assume that we are unable to frequently and accurately estimate the GOR of the well and rely on the historical data of well testing using test separator to obtain the GOR fluctuation range as the information we have. Therefore, in this case, we assume that based on well testing, this disturbance to fluctuate by up to $\pm 2.5\%$. If the disturbance increases by 2.5%, the optimal state is achieved when constraint (1e) is active. On the other hand, the optimal state is attained when constraint (1e) is inactive.

3. SELF-OPTIMIZING CONTROL STRUCTURE

This section provides a brief introduction to self-optimizing control, and its implementation on the problem described in Section 2. For a more detailed review of SOC, please refer to the survey paper by Jäschke et al. (2017).

3.1 General Principle

The goal of self-optimizing control (SOC) is to achieve near-optimal operation by controlling a combination of selected variables $\mathbf{c} \in \mathbb{R}^{n_\mathbf{u}}$ at their constant set points (Skogestad, 2000). The objective is to maintain these variables at their set-points despite the presence of varying disturbances, resulting in an acceptably low loss during operation. This is accomplished by utilizing feedback from the appropriate combination of measurements to counteract the effect of unmeasured disturbances d. It is important to note that this technique *assumes the same active constraints remain active for all values of the disturbances, and these constraints are controlled.*

This goal of this technique can be achieved through a heuristic method, null space method introduced by Alstad and Skogestad (2007), or a combination of them. In the following sections, several self-optimizing control structures applicable to a recirculated gas-lifted subsea oil production well are described. Constraints related to limited produced gas treatment capacity are considered.

3.2 Active Constraint Control

When the optimal set points remain unchanged, the position of the GLVs and the SCVs are typically maintained, which implies that the MVs remain constant at the values specified in Eq. 2. This configuration is referred to as *Structure 1*.

In this study, both the produced gas and surge line constraints are active at the nominal optimal operating point. To achieve effective control, the MVs (valve positions) should be paired with the constrained variables closely. This implies that the relationship between the constrained variables and MVs should have a high gain for better control, but the MVs' initial nominal optimal values should not readily lead to saturation in controlling the constraint. Therefore, manipulating GLV 3 to control the produced gas constraint (1e) is not recommended. Instead, we suggest using $z_{gl,5}$ (GLV 5) to control constraint (1e) as it has enough maneuvering room to handle the disturbance variation caused by GOR_2 increasing or decreasing by up to 2.5%. GLV 5 also has the highest gain compared to the remaining GLVs. This ensure effective control of active constraints which is essential, according to Skogestad (2000). This relationship can be expressed as

$$z_{gl,5} \rightarrow g(\mathbf{u}, d)$$

With respect to the gas-lift compressors, the most efficient operating point is achieved when the surge constraints (1d) are active. Although the SCVs are already saturated (fully closed) at the nominal optimal, in some cases, opening the SCV is necessary to ensure that the surge line constraint remains active. In other cases, when the SCV is fully closed (and already saturated), the discharge pressure of the gas lift compressor train is automatically adjusted, and the discharge pressure is considered floating and will never be saturated. As a result, we propose pairing the SCV with the associated surge line constraint (1d), which can be expressed mathematically as

$$z_{s,i} \rightarrow g_{z_{s,i}}(\mathbf{u}, d)$$

for $i = 1, 2, 3$. By incorporating these active constraint controllers, we refer to this configuration as *Structure 2*.

3.3 Heuristic Method

Active constraint set changing: The gas production of a reservoir can fluctuate due to various factors, such as the gas-oil-ratio (GOR). When well 2 produces more gas from the reservoir, as indicated by the increase in parameter GOR_2, the active constraint controller adjusts the position of GLV 5 for maximum produced gas handling capacity. This ensures no steady-state violation on the produced gas constraint (1e). However, if the amount of gas produced by well 2 decreases, the calculated position of GLV 5 from the active constraint controller may become unsuitable (active constraint set changes), *rendering the assumption of self-optimizing control invalid.* In such cases, it is necessary to identify an alternative self-optimizing controlled variable that is good and measurable for GLV 5. The position of GLV 5 itself is an obvious option. According to Krishnamoorthy and Skogestad (2020), we can choose the type of the selector based on the relationship between the MV and the constrained variables, and the suitable selector for this case is `MIN` selector. Additionally, we assume that the active surge constraint (1d) is the best choice for all values of expected disturbance.

When selecting a self-optimizing controlled variable, it is also important to consider its proximity to the source of the disturbance, which, in this case, is GOR_2. One option for stabilization is to use a readily available and measured variable, such as the bottom hole pressure of well 2, which is commonly used to stabilize the reservoir. Thus, the position of GLV 2 can be replaced with the bottom hole pressure of well 2 ($z_{gl,2} \rightarrow p_{bh,2}$). However, the bottom hole pressure may not always be a practical variable to measure, as damage to the associated sensor may require costly replacements due to its location. As an alternative, we can use wellhead pressure ($z_{gl,2} \rightarrow p_{wh,2}$), which is

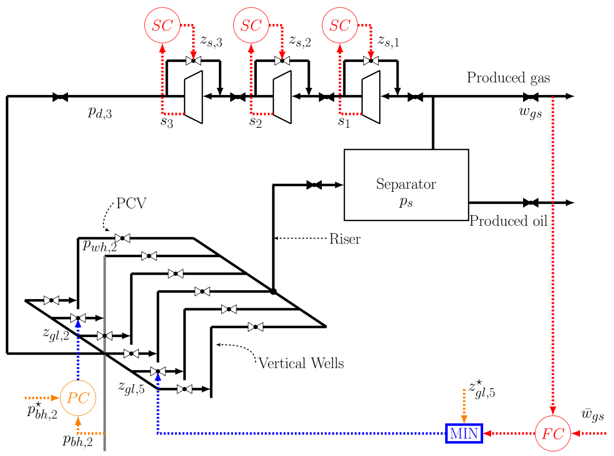

Fig. 2. *Structure 1* removes all controllers and selector, while *Structure 2* removes the pressure controller and selector, leaving only the online produced gas flow controller and surge controllers. *Structure 3* considers a `MIN` selector that allows the active constraint to change with $z_{gl,5}$ as the self-optimizing controlled variable when GOR_2 decreases, and $p_{bh,2}$ as another self-optimizing controlled variable for stabilization purposes. *Structure 4* considers wellhead pressure of well 2 ($p_{wh,2}$) instead of $p_{bh,2}$, and *Structure 5* considers the differential pressure of well 2 ($\Delta p_{bw,2} = p_{bh,2} - p_{wh,2}$) instead of $p_{bh,2}$. Black valves represent pressure drops.

easier to maintain and replace, although it may not be the closest variable to the source of the disturbance.

Another possible self-optimizing controlled variable is the differential pressure between wellhead and bottom hole pressure, which can be used to maintain the flow rate from the well by keeping the differential pressure constant. This can be performed by embedding an observer that considers all necessary pressure profile in the well to establish analytical redundancy if the sensor in the bottomhole underperforms.

Based on these heuristic steps, we construct three potentially promising control structures, named *Structure 3, 4, and 5*, as illustrated in Fig. 2. However, this heuristic method does not explore other measurement sets and remaining MVs, which may be impractical and time-consuming. This is the limitation of heuristic method.

3.4 Null Space Method

Combining different measurements can result in a better performing control structure. To incorporate unexplored measurements and MVs in a systematic way, we use the null space method. Let us assume that we have $n_{\mathbf{u}}$ independent unconstrained free variables $\mathbf{u}$, $n_{\mathbf{d}}$ independent disturbances $\mathbf{d}$, and $n_{\mathbf{y}}$ independent measurements $\mathbf{y}$. Our goal is to obtain $n_{\mathbf{c}} = n_{\mathbf{u}}$ independent controlled variables $\mathbf{c}$ that are linear combinations of the measurements, which can be expressed as: $\mathbf{c} = \mathbf{H}\mathbf{y}$.

To achieve this, we use the optimal sensitivity matrix

$$\mathbf{F} = \frac{\partial \mathbf{y}^{\star}}{\partial \mathbf{d}}$$

which is evaluated with constant active constraints. If $n_{\mathbf{y}} \geq n_{\mathbf{u}} + n_{\mathbf{d}}$, we can select the matrix $\mathbf{H}$ in the left null space of $\mathbf{F}$, such that $\mathbf{HF} = \mathbf{0}$. This choice of $\mathbf{H}$ ensures that fixing $\mathbf{c}$ at its nominal optimal value is first-order optimal for disturbances $\mathbf{d}$, resulting in zero loss as long as the sensitivity matrix $\mathbf{F}$ remains unchanged (Alstad and Skogestad, 2007). However, to prevent unnecessary complexity and cost, the number of measurements used in the structure should be limited. Ideally, a cost-benefit analysis should be performed to determine the optimal instrumentation for the plant.

Furthermore, null space method still assumes that the same active constraints remain active for all values of the disturbances. To *relax* this assumption into the design, we use a selector for active constraint switching. Similar to the heuristic method, we choose $z_{gl,5}$ as the self-optimizing controlled variable when GOR_2 decreases, using the `MIN` selector. This strategy eliminates the need to explicitly estimate GOR_2. Instead, any variation in GOR_2 is indirectly detected through changes in the total produced gas w_{gs}, which serves as the CV. The selector is determined by the relationship between MV and CV, as described by Krishnamoorthy and Skogestad (2020). Moreover, when the well is equipped with an adequate measurement set, it becomes feasible to estimate GOR_2 using a straightforward model or data processing techniques.

Ideally, we can implement null space method for unconstrained case, and construct another control structure for this case. This control structure can also be switched using selector (Jäschke et al., 2017). However, the optimal operating point of the other case is normally unknown in practice. Therefore, an insight from previous heuristic method is necessary.

Utilizing single MV (Structure 6): In addition to *flexible* active constraint controls (that is combined with `MIN` selector), this structure (denoted as *Structure 6*) consider the following measurement set: $\mathbf{y} = [p_{bh,2}\ p_{wh,2}]^{\top}$.

It is possible to replace one of the measurements with the position of GLV 2. However, doing so would result in a loss of control over either the bottom hole or wellhead pressure, which is undesirable as maintaining proper stabilizing control is crucial. Here, $z_{gl,2}$ is considered as an MV for stabilizing control.

To obtain the sensitivity matrix $\mathbf{F}$, numerical methods were employed. The null space method was then utilized to determine the optimal matrix $\mathbf{H}$, which corresponds to the following controlled variables:

$$c = 0.521 p_{bh,2} + 0.854 p_{wh,2} \tag{3}$$

This structure has the same measurement elements as *Structure 3-5*. Hence, comparing them is justified.

Based on branch and bound algorithm (Kariwala and Cao, 2009) and the requirement to keep at least either $p_{bh,2}$ or $p_{wh,2}$ as one of the measurements, we found that *Structure 6* is still the best option.

Utilizing two MVs (Structure 7): As we consider two MVs (i.e., $z_{gl,2}$ and $z_{gl,4}$) and one disturbance ($n_{\mathbf{d}} = 1$), three measurement is required ($n_{\mathbf{y}} = 3$). Further, as we have four measurement candidate and we want to include at least either $p_{bh,2}$ or $p_{wh,2}$ in the measurement set, four combinations of measurements need to be evaluated.

Unfortunately, the branch and bound algorithm (Kariwala and Cao, 2009) is not applicable because $z_{gl,4}$ may be saturated when GOR_2 increases up to 2.5%. Therefore, the only possible evaluation technique to determine the best combination is the average steady-state lost. Based on this technique, we found the best combination of measurement is: $\mathbf{y} = [p_{bh,2}\ p_{wh,2}\ p_{d,3}]^\top$, and the corresponded controlled variables are:

$$\mathbf{c} = \begin{bmatrix}\mathbf{c}(1)\\ \mathbf{c}(2)\end{bmatrix} = \begin{bmatrix}0.520p_{bh,2} + 0.854p_{wh,2} - 0.012p_{d,3}\\ 0.041p_{bh,2} - 0.012p_{wh,2} + 0.999p_{d,3}\end{bmatrix} \quad (4)$$

Based on Relative-Gain-Array (RGA) analysis (Skogestad and Postlethwaite, 2005), the recommended pairing is: $z_{gl,2} \to \mathbf{c}(1)$, and $z_{gl,4} \to \mathbf{c}(2)$.

4. RESULTS AND DISCUSSIONS

4.1 Estimated Loss Evaluation

One of the motivation of utilizing SOC is numerical robustness issues. In this simulation, we evaluate problem (1) with eleven (11) different value of GOR_2 ranging from 97.5% to 102.5% of GOR_2 nominal with 0.5% interval. The plant simulator is developed using the `CasADi ver. 3.5.1` toolbox (Andersson et al. (2019)) in `MATLAB R2019b` and is simulated using the `IDAS` integrator. The simulations are performed on a `2.11 GHz` processor with `16 GB` memory. The solver used is `IPOPT` with `MUMPS` as linear solver. Note that there are many linear solvers available and each has its own numerical limitation (Tasseff et al., 2019). Table 1 shows solver's performance, indicating that the solver is not always possible to obtain optimal solutions due to various numerical issues. For those cases, we estimate the optimal solutions based on the linear regression from the closest available two solution points. Thus, we consider *an optimal profit set* containing the solver-based optimal profit and the estimated optimal profit.

Steady-state loss is the difference between the profit obtained by the discussed/proposed control structure and the optimal profit from *the optimal profit set*. Table 2 summarizes steady-state loss obtained by different control structures when GOR_2 increases or decreases up to 2.5%.

Table 1. Solver's success and fail performance

−2.5%	−2.0%	−1.5%	−1.0%	−0.5%
✓	✗	✓	✓	✓
0.5%	**1.0%**	**1.5%**	**2.0%**	**2.5%**
✓	✓	✓	✗	✗

Table 2. Steady-state monthly loss

Control Structure	−2.5% GOR_2	+2.5% GOR_2 (est.)
1	NOK 59.544	Inf
2	NOK 6.116.745	NOK ∼ 3.444.831
3	NOK 604.897	NOK ∼ 2.810.376
4	NOK 686.095	NOK ∼ 3.595.481
5	NOK 633.027	NOK ∼ 3.065.285
6	NOK 124.246	NOK ∼ 1.523.036
7	NOK 248.667	NOK ∼ 1.817.930

4.2 Active Constraint Control

Structure 1 lacks a control strategy to handle reservoir uncertainty. This option is not ideal because an increase in GOR_2 leads to an increase in the amount of total

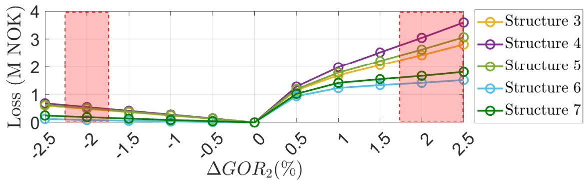

Fig. 3. Comparison of steady-state monthly loss of different structures. Red boxes indicates estimated loss evaluation.

produced gas. In steady-state, this violates the maximum gas handling capacity constraint. By installing constraint controllers, described in *Structure 2*, these violations are successfully eliminated. However, it is worth noting that the expected steady-state loss when GOR_2 decreases is much higher compared to *Structure 1* (see Table 2).

4.3 Heuristic Method

When GOR_2 decreases, in *Structure 3-5*, the self-optimizing controlled variable for GLV 5 is the position of the GLV 5, while the SCVs handle the surge constraints. As a result, *Structure 3-5* has successfully decreased the expected average steady-state loss compared to *Structure 2* (see Table. 2). In general, *Structure 3* outperforms other heuristic-based structures.

Depending on the reservoir dynamics and the possible controlling tuning, each control structure may reach the steady-state with different time steps/time constant. In addition to that, the selection of control structure should also consider the specific situation and constraints of the field. If immediate stabilization action is required and there is a reliable bottomhole sensor, *Structure 3* would be a good option. On the other hand, if maintaining the wellhead pressure is more feasible than installing and maintaining a bottomhole sensor, *Structure 4* may be preferable. *Structure 5* requires both a bottomhole and wellhead pressure sensor and is only viable if both sensors are functional.

The heuristic method is an intuitively useful tool for engineers. For instance, providing alternative self-optimizing controlled variable for GLV 5 when GOR_2 decreases is determined heuristically. This is significant considering null space method assumes the same active constraint for any disturbance values. While this method may provide valuable insights, it can also require significant effort and resources to achieve meaningful results. Therefore, it is essential to carefully consider the benefits and drawbacks of using the heuristic method in each specific situation, taking into account factors such as the scope of the problem, available resources, and the desired outcome.

4.4 Null Space Method

As expected, with the same element of measurement set, *Structure 6* outperforms control *Structure 3-5*, developed heuristically (see Fig. 3). When we consider more candidate of measurement, and utilize branch and bound algorithm to find the optimal measurement set, we found that *Structure 6* still outperforms other possible control structures, containing *artificial boundaries*, i.e, separator pressure and discharge compressor pressure. This is an essential result to demonstrate the importance of eliminating *artificial boundaries.*

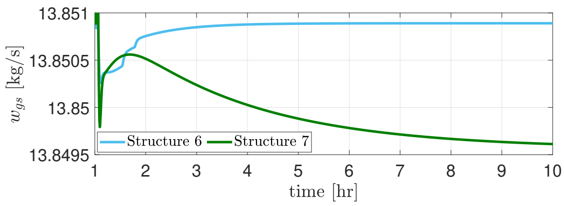

Fig. 4. Comparison of transient performance of *Structure 6* and *Structure 7* (consider $p_{d,3}$ in the measurement combination)

Increasing the number of the use of measurement set ($n_{\mathbf{y}} = 3$ in *Structure 7*) may not always leading to lower steady-state loss than *Structure 6*, for instance, if the additional used MV is saturated (see Fig. 3). In addition, null space method may maximize the use of available MVs by providing more measurement but it does not take into account the effect of the location of the suggested measurement element. For instance, *Structure 7* has discharge pressure in the measurement set which is located far away from its MVs (GLVs). As a consequence, it consumes more time in reaching the steady-state, as shown in Fig. 4. This comparison obtained with controller tuned using Simple IMC rule (Skogestad, 2003).

5. CONCLUSION

This paper investigated the possibilities of applying self-optimizing control to a recirculated gas lifted subsea oil well production optimization. This study reconfirms the previous work that self-optimizing control can be an alternative for optimization strategy without solver.

It was found that the most recommended control structure is *Structure 6*. This structure uses null space method in determining the optimal combination of controlled variables, uses a selector to allow active constraint region switching, and consider a required stabilizing control. This concludes that both heuristic and null space method are necessary and comply one to another.

As future works, we suggest considering cascade controller to solve the issue of having saturated MVs. In addition, it is also interesting design a control structure for a more realistic case where the surge constraint may be inactive, measurable GOR (including using embedded observer), multiple significant disturbances, and PCVs as manipulated variables.

REFERENCES

Aamo, O., Eikrem, G., Siahaan, H., and Foss, B. (2005). Observer design for multiphase flow in vertical pipes with gas-lift—theory and experiments. *Journal of Process Control*, 15(3), 247–257. doi: 10.1016/j.jprocont.2004.07.002.

Alstad, V. and Skogestad, S. (2007). Null Space Method for Selecting Optimal Measurement Combinations as Controlled Variables. *Industrial & Engineering Chemistry Research*, 46(3), 846–853.

Andersson, J., Gillis, J., Horn, G., Rawlings, J.B., and Diehl, M. (2019). CasADi: a software framework for nonlinear optimization and optimal control. *Mathematical Programming Computation*, 11, 1–36.

Backi, C.J., Grimes, B.A., and Skogestad, S. (2018). A Control- and Estimation-Oriented Gravity Separator Model for Oil and Gas Applications Based upon First-Principles. *Industrial & Engineering Chemistry Research*, 57(21), 7201–7217. doi:10.1021/acs.iecr.7b04297.

Cortinovis, A., Ferreau, H., Lewandowski, D., and Mercangöz, M. (2015). Experimental evaluation of MPC-based anti-surge and process control for electric driven centrifugal gas compressors. *Journal of Process Control*, 34, 13–25. doi:10.1016/j.jprocont.2015.07.001.

Elldakli, F. (2017). Gas Lift System. *Petroleum & Petrochemical Engineering Journal*, 1(3). doi: 10.23880/PPEJ-16000121.

Gravdahl, J. and Egeland O. (1998). *Compressor Surge and Rotating Stall: Modeling and Control*. Springer.

Jäschke, J., Cao, Y., and Kariwala, V. (2017). Self-optimizing control – A survey. *Annual Reviews in Control*, 43, 199–223. doi:10.1016/j.arcontrol.2017.03.001.

Kariwala, V. and Cao, Y. (2009). Bidirectional branch and bound for controlled variable selection. Part II: Exact local method for self-optimizing control. *Computers & Chemical Engineering*, 33(8), 1402–1412. doi: 10.1016/j.compchemeng.2009.01.014.

Krishnamoorthy, D., Foss, B., and Skogestad, S. (2016). Real-Time Optimization under Uncertainty Applied to a Gas Lifted Well Network. *Processes*, 4(4), 52. doi: 10.3390/pr4040052.

Krishnamoorthy, D., Foss, B., and Skogestad, S. (2018). Steady-state real-time optimization using transient measurements. *Computers & Chemical Engineering*, 115, 34–45. doi:10.1016/j.compchemeng.2018.03.021.

Krishnamoorthy, D. and Skogestad, S. (2020). Systematic design of active constraint switching using selectors. *Computers & Chemical Engineering*, 143, 107106. doi: 10.1016/j.compchemeng.2020.107106.

Matias, J.O. and Le Roux, G.A. (2018). Real-time Optimization with persistent parameter adaptation using online parameter estimation. *Journal of Process Control*, 68, 195–204. doi:10.1016/j.jprocont.2018.05.009.

Mehdizadeh, P. (2007). Worldwide Multiphase and Wet Gas Metering Installations. Technical report, Production Technology Report.

Milosavljevic, P., Marchetti, A.G., Cortinovis, A., Faulwasser, T., Mercangöz, M., and Bonvin, D. (2020). Real-time optimization of load sharing for gas compressors in the presence of uncertainty. *Applied Energy*, 272, 114883. doi:10.1016/j.apenergy.2020.114883.

Skogestad, S. (2000). Plantwide control: the search for the self-optimizing control structure. *Journal of Process Control*, 10(5), 487–507. doi:10.1016/S0959-1524(00)00023-8.

Skogestad, S. (2003). Simple analytic rules for model reduction and PID controller tuning. *Journal of Process Control*, 13(4), 291–309. doi: https://doi.org/10.1016/S0959-1524(02)00062-8.

Skogestad, S. and Postlethwaite, I. (2005). *Multivariable Feedback Control*. John Wiley and Sons, New York, NY, USA.

Tasseff, B., Coffrin, C., Wachter, A., and Laird, C.D. (2019). Exploring Benefits of Linear Solver Parallelism on Modern Nonlinear Optimization Applications. *arXiv: Optimization and Control*.